OPEN ACCESS Freely available online

PLOS ONE

Inhibition of the Water Oxidizing Complex of Photosystem II and the Reoxidation of the Quinone Acceptor Q_A^- by Pb^{2+}

Ahmed Belatik, Surat Hotchandani, Robert Carpentier*

Groupe de Recherche en Biologie Végétale, Université du Québec à Trois-Rivières, Trois-Rivières, Québec, Canada

Abstract

The action of the environmental toxic Pb^{2+} on photosynthetic electron transport was studied in thylakoid membranes isolated from spinach leaves. Fluorescence and thermoluminescence techniques were performed in order to determine the mode of Pb^{2+} action in photosystem II (PSII). The invariance of fluorescence characteristics of chlorophyll a (Chl a) and magnesium tetraphenylporphyrin (MgTPP), a molecule structurally analogous to Chl a, in the presence of Pb^{2+} confirms that Pb cation does not interact directly with chlorophyll molecules in PSII. The results show that Pb interacts with the water oxidation complex thus perturbing charge recombination between the quinone acceptors of PSII and the S_2 state of the Mn_4Ca cluster. Electron transfer between the quinone acceptors Q_A and Q_B is also greatly retarded in the presence of Pb^{2+}. This is proposed to be owing to a transmembrane modification of the acceptor side of the photosystem.

Citation: Belatik A, Hotchandani S, Carpentier R (2013) Inhibition of the Water Oxidizing Complex of Photosystem II and the Reoxidation of the Quinone Acceptor Q_A^- by Pb^{2+}. PLoS ONE 8(7): e68142. doi:10.1371/journal.pone.0068142

Editor: Rajagopal Subramanyam, University of Hyderabad, India

Received April 26, 2013; **Accepted** May 24, 2013; **Published** July 4, 2013

Funding: This work is supported by a grant from Natural Sciences and Engineering Research Council of Canada (NSERC). The funders had no role in study design, data collection and analysis, decision to publish, or preparation of the manuscript.

Competing Interests: The authors have declared that no competing interests exist.

* E-mail: Robert.Carpentier@uqtr.ca

Introduction

Heavy metals play essential cofactor roles as structural and catalytic components of enzymes in many physiological processes required for the normal development of plants. Over the course of evolution, plants have developed different mechanisms that control and respond to the intake and accumulation of both essential and nonessential heavy metals. However, some heavy metals such as lead can be highly toxic to cells and cell organelle functions even at very low concentrations. Although the influence of excessive dose of heavy metals on the photosynthetic activity of plants has been studied in many cultivated species (1–3), the mechanism of heavy metal toxicity on photosynthesis is still a matter of great debate. Some evidence points to their involvement as inhibitors of electron transport in light reactions (4–5) and in the inhibition of enzyme activity in dark reactions by the direct blocking of protein functions or displacement of endogenous metals (6–7).

Lead, found in the environment, comes from both natural and anthropogenic sources. The metal is present in the soil, but also in all other environmental compartments: water, air and even living beings (8). The toxicity of a metal depends on its chemical state as well as on environmental factors (9–10). In soil, Pb can be found in ionic form, or bound to the soil particles (11). It has two oxidation states, namely 2^+ and 4^+. The tetravalent state is a strong oxidant but is not abundant in the environment. The divalent state, on the other hand, is more stable and prominent in the environment (12). The accumulation of Pb from atmospheric deposition or contaminated waste is largely stored in the soil, mainly in the surface layers and, more specifically, in the organic-rich layers (13). However, a small fraction of the metal is also absorbed by living organisms (micro-and meso-organisms, plants …etc.).

The photosystem II (PSII) complex is one of the two membrane-bound large multisubunit chlorophyll–protein complexes (PSII and PSI) of plants, algae and cyanobacteria embedded in the thylakoid membranes. PSII collects light energy, converts it into electro-chemical energy and drives electron transfer from water to PSI. On its acceptor side, PS II electron transport involves two acceptor quinones, Q_A and Q_B that are arranged around a non-heme iron. This non-heme iron is hexacoordinated by four histidines and two remaining ligand positions are taken by the oxygen atoms of bicarbonate as bidentate ligand (14–15). Further, the study of the effect of bicarbonate has suggested that the non-heme iron plays a role of an electron- transport regulator on the acceptor side of PSII. Although the precise mechanism of this process needs more study, the depletion of bicarbonate results in a decelerating of the electron transfer rate between Q_A and Q_B (16–20). The water oxidation complex (WOC) is located on the donor side of PSII. It is composed of a Mn_4Ca cluster where the successive absorption of four quanta by PSII results in the advancement of the S-states cycle from $S_0 \rightarrow S_1 \rightarrow S_2 \rightarrow S_3 \rightarrow (S_4) \rightarrow S_0$. The S_4-state decays to the S_0-state after the 4^{th} flash with the concurrent oxygen evolution. The electrons are passed from the WOC to the reaction center $P680^+$ through the secondary electron donor, Tyr_Z (Tyrosine 161 of D1 subunit) (21).

At present, there are only a few reports regarding the adverse action of Pb^{2+} on the photosynthetic apparatus (22 and references therein). A decline of the photochemical quantum yield of PSII was observed in isolated thylakoid membranes from spinach (23). It was proposed that Pb^{2+} affects oxygen evolution by removing

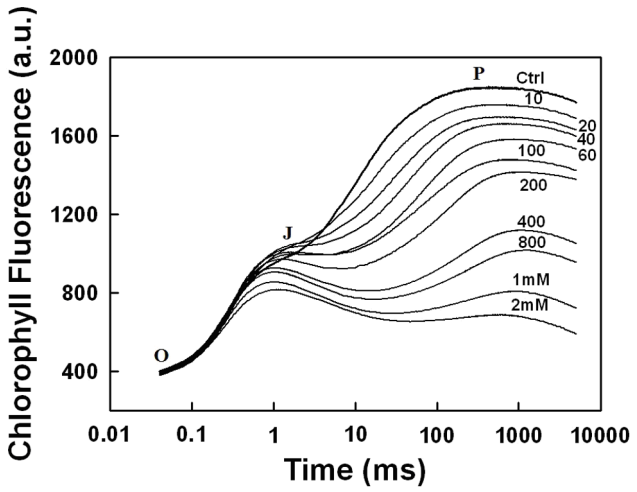

Figure 1. Typical traces of Chl a fluorescence rise in isolated thylakoid membranes in the absence (Ctrl) or in the presence of $PbCl_2$ added in various concentrations (μM, unless specified in mM) as indicated by numbers adjacent to traces. See Materials and methods for details.
doi:10.1371/journal.pone.0068142.g001

extrinsic polypeptides and/or Ca^{2+} or Cl^- ions associated with the water oxidizing complex of PSII (5, 24). Lead cation was also recently shown to affect PSI electron transport presumably due to binding near or at plastocyanin (25).

In this study, we have further investigated the mechanism of the action of Pb^{2+} in thylakoid membranes. The effects of the metal ion on the electron transport were studied using thermoluminescence and fluorescence spectroscopic techniques. Functional assays were used to determine the site of action and consequences of metal ion interaction in the thylakoid membranes and to explore the mode of action of the metal that causes the loss of photosystem II functions.

Materials and Methods

Thylakoid Membranes Isolation

Thylakoid membranes were prepared from fresh market spinach leaves (*Spinacia oleracea* L.) as described elsewhere (26), and were stored in the dark in 50 mM Hepes NaOH (pH 7.6), 0.33 M sorbitol, 2 mM EDTA, 1 mM $MgCl_2$, 1 mM NaCl, and 10 mM KCl.

Chlorophyll Fluorescence Induction

Chlorophyll *a* fluorescence induction (FI) measurements were performed at room temperature using the Plant Efficiency Analyser (Hansatech, King' Lynn, Norfolk, UK). The assay medium consisted of 50 mM Hepes-NaOH (pH 7.6), 0.33 M sorbitol, 2 mM EDTA, 1 mM $MgCl_2$, 1 mM $MnCl_2$, 10 mM KCl, and 10 mM NaCl with a final Chl concentration of 25 μg mL^{-1} for thylakoid membranes. Red excitation light peaking at

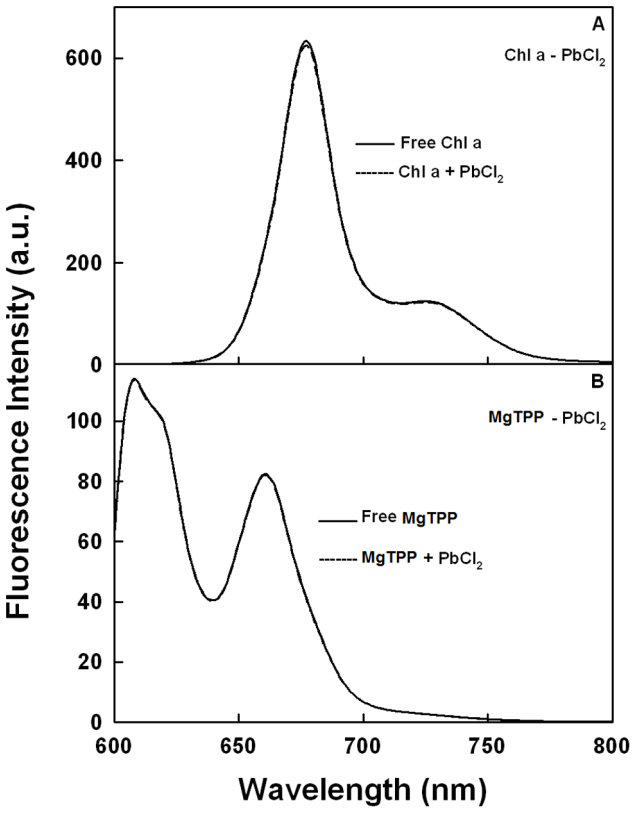

Figure 2. Fluorescence emission spectra of: (A) ethanolic solution of Chl a (2.5 μM) alone (−) and in presence of 1 mM $PbCl_2$ (–); (B) ethanolic solution of MgTPP (2.5 μM) alone (−) and in presence of 1 mM $PbCl_2$ (–). In both cases, the excitation wavelength was 433 nm.
doi:10.1371/journal.pone.0068142.g002

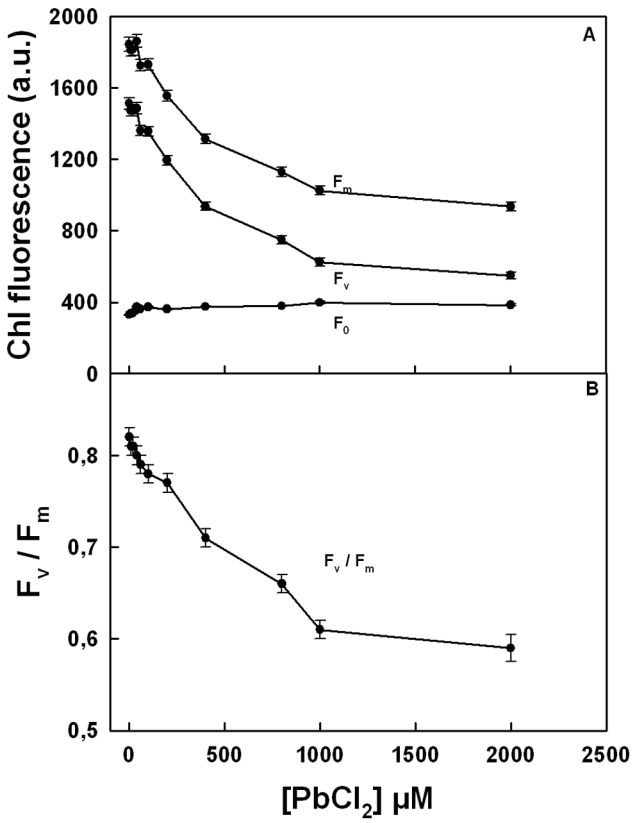

Figure 3. Effect of various concentration of $PbCl_2$ on Chl fluorescence induction parameters in thylakoids membranes. (A) F_m, F_v and F_0, *vs* $PbCl_2$ (B) F_v/F_m *vs* $PbCl_2$. Each point is the average of nine experiments.
doi:10.1371/journal.pone.0068142.g003

Table 1. Effect of $PbCl_2$ on the relative amplitude (A) and half-life time ($t_{1/2}$) of the exponential decay components of Chl a fluorescence yield after a single turnover flash measured in thylakoid membranes in the absence and in the presence of 50 μM DCMU.

Without DCMU $PbCl_2$ (μM)	**Fast Phase**		**Middle Phase**		**Slow Phase**	
	$t_{1/2}$ (±10 μs)	**A (±5%)**	**$t_{1/2}$ (±0.3 ms)**	**A (±3%)**	**$t_{1/2}$ (0.4 s)**	**A (±2%)**
0	430	69	6.1	22	5.9	9
10	690	61	7.5	26	7.1	13
100	987	45	11.3	35	12.1	20
1000	1440	28	16.8	43	15.6	29
2000	1590	19	18.2	46	17.2	35
With DCMU $PbCl_2$ (μM)	**Fast Phase**		**Middle Phase**		**Slow Phase**	
	$t_{1/2}$ (±5 ms)	**A (±4%)**	**$t_{1/2}$ (±0.03 s)**	**A (±3%)**	**$t_{1/2}$ (±0.3 s)**	**A (±2%)**
0	298	41	1.79	47	18.5	12
10	1130	26	1.92	53	22.1	21
100	1560	19	2.25	58	23.6	23
1000	–	–	4.35	68	31.2	32
2000	–	–	4.86	69	31.9	31

doi:10.1371/journal.pone.0068142.t001

655 nm with an intensity of 1800 μmol m^{-2} s^{-1} was obtained from six light emitting diodes. As the fluorescence signal during the first 40 μs is ascribed to artifacts due to a delay in response time of the instrument, these data were not included in the analysis of FI traces.

Thermoluminescence

Measurements of thermoluminescence were performed using home-built equipment. The complete description of the design and functional aspects are described elsewhere (27–28). Thylakoid membranes were diluted to a final Chl concentration of 200 μg mL^{-1} in a medium containing 50 mM Hepes-NaOH (pH 7.6), 0.33 M sorbitol, 2 mM EDTA, 1 mM $MgCl_2$, 1 mM $MnCl_2$, 10 mM KCl, and 10 mM NaCl. About 300 μL of the suspension was added to the sample compartment (15 mm diameter) positioned just above Peltier plate and covered with a Hellma 202-OS disc window. The sample chamber was closed with a holder bearing the light guide connected to the photomultiplier. The sequence of incubation periods and flash illumination was as follows. The samples were pre-incubated for 120 s at 20°C. Then the temperature was brought down to 2°C within 36 s and kept for 60 s**.** Two actinic single turn-over saturating white flashes of about 2 μs pulse width (setting 10, XE-STC, Walz, Germany) were then applied to initiate charge separation in PSII. Finally, a linear warming (0.5°C s^{-1}) of the samples in total darkness activated the recombination of PSII charge pairs that can be detected by the appearance of emission bands with characteristic temperature optima (27–28).

Fluorescence Measurements

Fluorometric experiments were carried out at room temperature 24°C with a Perkin Elmer LS55 Spectrometer equipped with a red-sensitive photomultiplier R928. Samples were excited at 434 nm and fluorescence emission spectra were measured from 600 to 800 nm as described by Rajagopal et al (2003) (29). The excitation and emission spectral widths were fixed at 5 and 2.5 nm, respectively, and emission spectra were corrected according to the photomultiplier sensitivity using the correction factor spectrum provided by Perkin-Elmer.

Flash-induced Fluorescence Decay Kinetics

In order to examine the reduction and oxidation kinetics of Q_A, Chl fluorescence rise and its relaxation in the dark were measured with FL3500 Fluorometer (Photon Systems Instruments, Brno, Czech Republic) as described previously (30–31). Thylakoid membranes (Chl concentration of 25 μg ml^{-1}) were incubated for 3 min at room temperature in complete darkness without or with 50 μM of DCMU before initiating the fluorescence measurements. Samples were excited with a 20 μs red actinic flash from a LED peaking at 625 nm and prompt fluorescence was measured for 1 min. The first measurement was taken 20 μs after the flash was given. The traces were averaged to estimate the half-life times and amplitudes of the fluorescence decay components using the following three exponential functions:

$$F(t) = F' + A_1 e^{-K_1 t} + A_2 e^{-K_2 t} + A_3 e^{-K_3 t} \quad (1)$$

where F(t) is the fluorescence value at time t, k_n is the rate constant, A_n is the amplitude of the fluorescence relaxation phase, and F′ is the stable minimal fluorescence at the end of the decay.

Results

Chlorophyll Fluorescence Induction

The kinetic curves of the fast Chl fluorescence rise were measured in isolated thylakoid membranes both untreated and those treated with various concentrations of $PbCl_2$ as shown in Fig. 1. The FI traces, normalized at minimal values (F_0), are characterized by a series of inflections in the rate of rise in the fluorescence intensity termed as OJIP transient (32–33). In isolated thylakoid membranes, the I step of the OJIP fluorescence, as observed by Bukhov et al 2003 (34), cannot be resolved visually

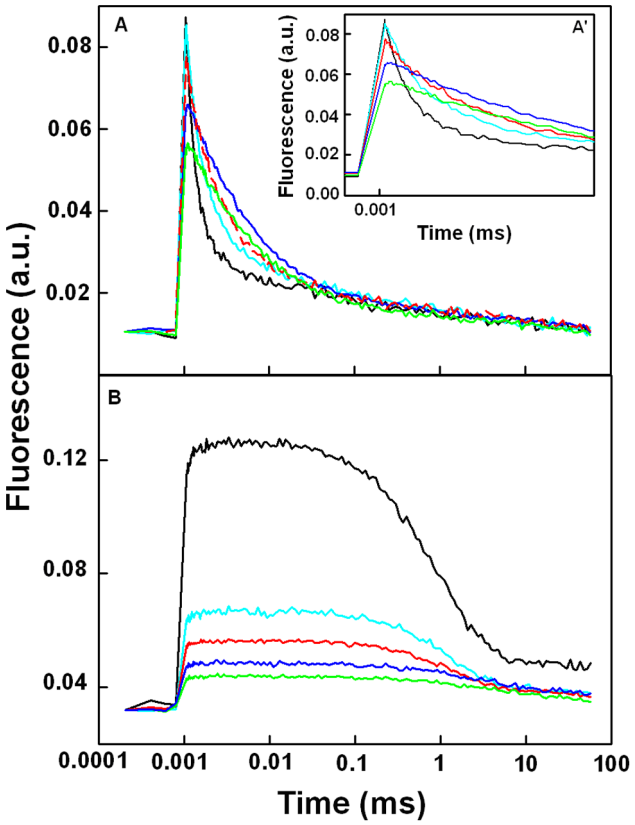

Figure 4. Effect of $PbCl_2$ on the relaxation of single turnover flash-induced Chl fluorescence yields in thylakoids membranes with different lead concentrations: 0 (black), 10 (sky blue), 100 (red), 1000 (blue) and 2000 μM (green). The measurements were performed in the absence (A) or in the presence (B) of 50 μM DCMU and all the traces were normalized. Each trace is the average of ten experiments.
doi:10.1371/journal.pone.0068142.g004

due to the significant overlap between JI and IP phases (Fig. 1, Ctrl). However, Pospisil and Dau 2002 (35) and Boisvert et al 2006 (36) have decomposed the OJIP traces by fitting the experimental curves with a sum of three mono-exponential components. This

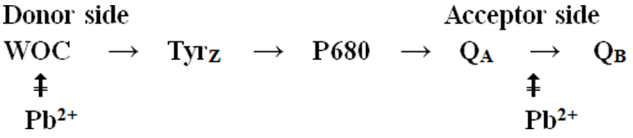

Figure 6. Schematic representation of the proposed inhibitory sites of Pb^{2+} in PSII.
doi:10.1371/journal.pone.0068142.g006

method showed a good fit of the OJIP traces with the three components OJ, JI and IP, even though the inflection step I was absent (36). The I step can be restored by the addition of some different exogenous electron acceptors at the Q_B site of PSII (37). The treatment with different concentrations (10–400 μM) of lead increased the relative fluorescence intensity at J step while the rise towards the P step was retarded and the fluorescence intensity at P declined (Fig. 1). This suggests that the electron transfer between Q_A^- and Q_B was slowed down with the increasing Pb^{2+} concentration. However, at Pb^{2+} concentrations greater than 400 μM, the OJ phase also began to decrease and the overall fluorescence induction was strongly damped (Fig. 1). Furthermore, the intensity of JIP phase also diminished with increased concentration of Pb cation. In other words, one observed a quenching of Chl fluorescence as the concentration of $PbCl_2$ increased.

Fluorescence of Chl a and MgTPP

The observed Chl fluorescence quenching (Fig. 1) may be the result of the direct interaction of $PbCl_2$ with the excited states of Chl of PSII thereby altering its radiative characteristics. Therefore, in order to verify this possibility, the fluorescence of Chl a in ethanolic solution was studied in absence and presence of $PbCl_2$ (Fig. 2A). The fluorescence of Chl a in this solution exhibits a maximum at 675 nm, which is characteristic of monomeric Chl a (38). As seen from the figure, the fluorescence properties of Chl a practically remained unchanged upon addition of $PbCl_2$. This suggests that $PbCl_2$ has no direct effect on the excited singlet states of Chl a, and thus on its radiative properties. To further confirm this observation, fluorescence studies of MgTPP were performed in the presence of Pb^{2+} (Fig. 2B). The use of MgTPP is due to its structural analogy with Chl a as it is composed of the same porphyrin macrocycle with central Mg. In addition, the added

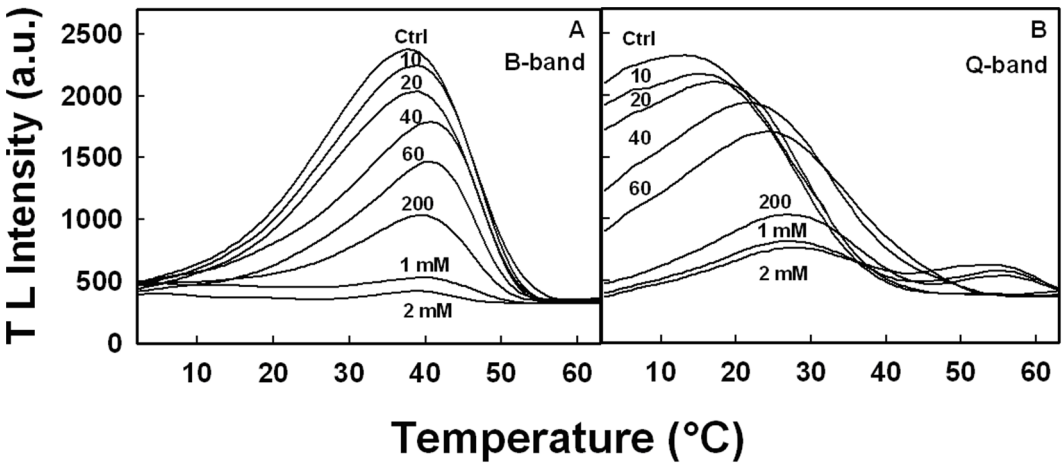

Figure 5. Thermoluminescence spectra measured in isolated thylakoid membranes in the absence (A) or presence of 50 μM DCMU. $PbCl_2$ was added in various concentrations (μM, unless specified in mM) as indicated by numbers adjacent to traces.
doi:10.1371/journal.pone.0068142.g005

advantage of using MgTPP is that it does not contain the phytol chain as is present in Chl a, and, as a result, can be more easily accessible to the additives. It is shown in Fig. 2B that $PbCl_2$ had no effect on the fluorescence properties of MgTPP thus confirming the results obtained with Chl a.

Chlorophyll Fluorescence Induction Parameters

The Chl fluorescence properties of thylakoid membranes in the presence of Pb^{2+} were further subjected to the comprehensive analysis of fluorescence induction kinetics (Fig. 3). The initial fluorescence F_0 (O-level), which describes the functional state of PSII reaction centers in terms of its openness in the dark-adapted state (39), remained virtually unchanged by the addition of Pb cations (Fig. 3A). However, in order to assess the effect of $PbCl_2$ on the maximum quantum yield of the primary photochemistry of PSII in thylakoid membranes, the changes in the maximal fluorescence observed in dark adapted samples, F_m, when the excitons have been trapped and all the reaction centers of PSII are in closed state (40), were also examined. As seen from Fig. 3A, F_m greatly diminished as Pb^{2+} concentration increased. This decline in Fm leads to a decrease in the variable fluorescence Fv (Fv = Fm - F_0) and, consequently, Fv/Fm, the maximal PSII photochemical quantum yield, also decreased (Fig. 3B). This decrease in Fv/Fm brings about a simultaneous decline in Fv/F_0 (result not shown), a parameter that accounts for the simultaneous variations in Fm and F_0 for the determination of the maximum photochemical quantum yield of PSII (41). Since, as noted in Fig. 3A, F_0 remains practically invariant with increasing Pb concentrations, the inhibitory effect of Pb^{2+} on the quantum yield of PSII photochemistry is, therefore, principally related to the changes in F_m.

Flash-induced Chl Fluorescence Decay Kinetics

The fluorescence induction traces (Fig. 1) indicated that the reoxidation of Q_A was affected in the presence of $PbCl_2$. This observation was further verified using the fluorescence properties of dark adapted isolated thylakoid membranes submitted to a single turnover flash and normalized at minimal values (Fig. 4A). The fluorescence rise induced by the flash is due to the reduction of Q_A, the primary quinone acceptor of PSII, and the decay thereafter in the dark is related to the reoxidation of Q_A^- and consists of several kinetic phases. The amplitude of the fluorescence rise greatly decreased when the concentration of $PbCl_2$ increased, especially at concentrations above 100 μM. In order to characterize quantitatively the fluorescence decay kinetics, the dark decay was fitted with three exponential components (Table 1). The fast component is attributed to the reoxidation of Q_A^- by Q_B (42–43), the middle component is ascribed to the Q_A^- reoxidation in PSII centers with an empty Q_B site and is limited by the diffusion time of PQ to the Q_B binding site. The slow phase is associated with the reoxidation of Q_A^- through charge recombination with the S_2 and/or S_3 states of the Mn_4Ca cluster (42–43). The amplitudes and the half-life times of the components are shown in Table 1. The amplitude of the fast phase greatly decreased with increasing amounts of $PbCl_2$, this was accompanied by a strong increase in the half-life time of all three components of the decay kinetics (Table 1).

The decay was also measured in the presence of DCMU that blocks electron transfer between Q_A^- and Q_B (Fig. 4B). In this case, the reoxidation of Q_A^- is owing to its charge recombination with the donor side of PSII. The fluorescence decay in the presence of DCMU can also be fitted with three exponential components (44–45). The fast component is due to the charge recombination with partially active Mn_4Ca clusters, the middle component arise from the recombination of $S_2Q_B^-$ charge pairs. The slowest component is associated with PSII with an oxygen evolving center in the S_0 state before the flash was applied. The amplitudes of the middle and slow components increased with $PbCl_2$ at the expense of the fast component and their half-life times increased (Table 1).

Thermoluminescence

Thermoluminescence was used to further explore the effects of $PbCl_2$ on charge recombination between donor and acceptor sides of PSII. The TL glow curves for untreated (Ctrl) and Pb^{2+}-treated thylakoid membranes following two single turn-over white flashes are displayed in Fig. 5A. The TL signal (Fig. 5A, Ctrl) attained its maximal intensity at the temperature of 38°C, characteristic of the temperature optimum for the B band appearing in the range between 30 and 40°C, as previously reported for this type of material (46–47). The B band is attributed to the charge recombination of $S_2/S_3Q_B^-$ pairs produced by linear electron transport in PSII (48–51). The intensity of the B band progressively diminished as the concentration of $PbCl_2$ increased (Fig. 5A). The addition of 20 μM $PbCl_2$ produced 13% decrease in TL intensity, and in the presence of 2 mM $PbCl_2$, the TL intensity was suppressed completely. Also, the decline of the band was accompanied by an upshift of the maximal temperature (Tm) from 38°C to 41°C.

The changes in the amplitude and Tm of the B band could be related to changes in the properties of the S_n states of the Mn_4Ca cluster and/or to modification of the Q_B binding site in the presence of $PbCl_2$. In order to elucidate the site of action of $PbCl_2$ in the electron transport chain, the TL glow curves were recorded following two single turn-over white flashes in the presence of 50 μM of PSII inhibitor DCMU, known to block the electron flow beyond Q_A. DCMU eliminated the B band with a simultaneous appearance of Q band with a maximum at 17°C, attributed to the back-flow of electrons from Q_A^- to the S_2-state (48–51) (Fig. 5B). The reason for the absence of B band is that since DCMU stops the electron flow past Q_A, the formation of Q_B^- and state S_3 is not realized (49). The addition of 20 μM $PbCl_2$ already suppressed 12% of the Q band intensity. A progressive decrease of the Q band was observed when the concentration of $PbCl_2$ was further increased. The addition of 2 mM $PbCl_2$ caused the loss of more than 90% of Q band intensity. This loss was accompanied by a strong upshift of Tm from 17°C to 27°C.

Discussion

The negative action of Pb^{2+} on PSII photochemistry and electron transport, uninfluenced by PSI activity, was studied in thylakoid membranes using various approaches specific for PSII. Chlorophyll fluorescence induction kinetics measurements (Fig. 1) have shown that the fluorescence was greatly quenched when $PbCl_2$ was added. Several authors postulated that damage caused by heavy metal ions (such as Zn^{2+}, Cu^{2+}, and Pb^{2+}) to plants was due to the substitution of the central Mg from the Chl a molecules thus causing fluorescence quenching (52–54, 22). However, measurements of pure Chl a or MgTPP fluorescence in ethanolic solution (Fig. 2) have demonstrated that the addition of $PbCl_2$ has no effect on the excited states of Chl a and the structure of the pigment remains intact. The fluorescence quenching observed during Chl fluorescence induction is, therefore, related to the modifications in the photochemical activity of PSII.

The OJIP traces constitute an essential tool to study the activity and integrity of the photosynthetic apparatus under different stress conditions, providing the information on PSII photochemistry such as the electron transport on both donor and acceptor sides of

the photosystem (32–33, 55). The IP step of the Chl fluorescence induction has been correlated with the photoreduction of the PQ pool (56–57). Thus, the observed decline in IP phase indicates a strong inhibition of the accumulation of reduced PQ especially at Pb^{2+} concentrations above 400 μM (Fig. 1). This coincided with a decrease in the Fv/Fm values due to a decrease in Fm (Fig. 3) (23). This part of the induction is known to be more sensitive to the unfavourable treatments in comparison with the photochemical phase (OJI) (58). Indeed, the perturbation in the structure-function relations of the WOC has been shown to correlate with the quenching of the IP fluorescence rise that results in a decline of Fm (36, 58). The above is in line with the previous reports showing that Pb^{2+} causes the release of extrinsic polypeptides associated with the WOC together with the Ca^{2+} and Cl^- required as cofactors (5, 25). Therefore, the inhibition of JIP rise and the more significant damping of the whole fluorescence induction kinetics above 400 μM Pb^{2+} are the result of the disorganization of the WOC causing the lack of electron flow towards the acceptor side of PSII. The damage of the Mn_4Ca cluster is also supported by the decline of both Q and B thermoluminescence bands. Such inhibition of both $S_2Q_A^-$ and $S_2Q_B^-$ charge recombination (Q and B band, respectively) shows that the S_2 state of the WOC becomes unavailable as the common recombination partner with increasing concentrations of $PbCl_2$ and indicates a dysfunction of the WOC.

On the other hand, the OJ phase is related to the reduction state of Q_A (56, 59). The relative increase of OJ in the presence of low concentrations of $PbCl_2$ (Fig. 1) is strongly indicative of a delayed electron transfer from Q_A^- to Q_B. This was indeed verified using the measurements of Chl fluorescence decay kinetics following a single turn-over flash (Fig. 4). The fluorescence decay was greatly retarded with the life-time of all three components being significantly increased even at concentrations below 400 μM $PbCl_2$ (Table 1). The amplitude of the fast component, attributed to electron transfer from Q_A^- to Q_B, diminished with a concurrent increase of the other components. Also, the decreased rate of Q_A^- reoxidation resulted in an increased amplitude of the slow component attributed to the back reactions with the S_2 state of the Mn_4Ca cluster (42–43). This corresponds with the increased amplitude of the middle component of the decay measured in the presence of DCMU (Table 1), a component also attributed to S_2/Q_A^- recombination (44–45). Therefore, the population of PSII centers with a reduced Q_A that is reoxidized through S_2/Q_A^- recombination is increased but the rate of this reoxidation is strongly declined most likely due to the stabilization of the S_2 state of the WOC (see below).

The delayed reoxidation of Q_A^- maybe interpreted in terms of an active site of Pb^{2+} being near Q_A or Q_B. Indeed, similar data were previously used to conclude that an inhibitory site of various metal cations was located between Q_A and Q_B (Fig. 6) (60–62). However, the destabilization of the WOC discussed above may also cause the delayed Q_A^- reoxidation. It was indeed shown that the removal of the extrinsic polypeptides or Ca^{2+} from the WOC can cause the diminished rate of Q_A^- reoxidation through a transmembrane conformational effect (42). Removal of Ca^{2+} from the WOC also produces a modification in the mid-point potential of Q_A thus altering the electron transfer process between Q_A and Q_B (63, 43). It can be postulated that this conformational change modifies the bicarbonate binding that is required for proper electron transfer from Q_A^- to Q_B (17, 18). Therefore, it is plausible that the action of Pb^{2+} at the WOC would cause this same transmembrane effect as was also proposed for the inhibitory action of Ni^{2+} and polyamines (64–65). This view is supported by the strong progressive upshift of the Tm of Q and B thermoluminescence bands with increasing concentrations of Pb^{2+} (Fig. 5). Such large increase in thermoluminescence temperature was previously associated with the stabilization of the S_2 state of the WOC due to the modification in the ligand environment of the Mn_4Ca complex following the depletion in Cl^- or in 33 kDa extrinsic polypeptide (66–67). Therefore, the shift of Tm towards higher temperatures may be due to a change in the population of PSII centers with a stabilized S_2 state owing to the action of Pb^{2+} causing a retarded Q_A^- reoxidation at low Pb^{2+} concentrations. This may represent an intermediate step in the inhibition of the WOC that precedes the serious damping of the fluorescence induction observed at high Pb^{2+} concentrations (Fig. 1).

Although an active site of Pb^{2+} at or near Q_B cannot be fully excluded, the negative action of Pb^{2+} is postulated to proceed in two steps. During the intermediate step, the environment of the Mn_4Ca complex is disorganized and the S_2 state of the WOC is stabilized which consequently affects Q_A^- reoxidation and increases S_2/Q_A^- charge recombination (though the recombination proceeds at a slower rate compared to the control). During the final phase, the WOC is damaged more seriously leading to a loss of charge recombination and of PQ reduction.

Author Contributions

Conceived and designed the experiments: AB RC. Performed the experiments: AB. Analyzed the data: AB SH RC. Contributed reagents/materials/analysis tools: SH RC. Wrote the paper: AB SH RC.

References

1. Prasad MNV, Strzałka S (1999) Impact of heavy metals on photosynthesis. In: Heavy Metal Stress in Plants, from Molecules to Ecosystems. Prasad MNV, Hagemeyer J, editors. Berlin: Springer. 117p.
2. Shaffer M (2001) Waste lands: the threat of toxic fertilizer. California's Advocate for the Public Interest Los Angeles CA.
3. Baker AJM, Walker PL (1990) Ecophysiology of metal uptake by tolerant plants, heavy metal tolerance in Plants. In: Shaw AJ. Evolutionary Aspects. CRC Press Boca Raton. 155–177.
4. Giardi MT, Masojidek J, Godde D (1997) Discussion on the stresses affecting the turnover of the D1 reaction center II protein. Plant Physiol 101: 635–642.
5. Rashid A, Camm EL, Ekramoddoullah KM (1994) Molecular mechanism of action of Pb^{2+} and Zn^{2+} on water oxidizing complex of photosystem II. FEBS Lett 350: 296–298.
6. Chugh LK, Sawhney SK (1999) Photosynthetic activities of Pisum sativum seedlings grown in presence of cadmium. Plant Physiol Biochem 37: 297–303.
7. Van Assche F, Clijsters H (1990) Effects of metals on enzyme activity in plants. Plant Cell Environ 13: 195–206.
8. Morlot M (1996) Aspects analytiques du plomb dans l'environnement, édition Lavoisier TEC&DOC.
9. Babich H, Stotzky G (1980) Environmental factors that influence the toxicity of heavy metals and gaseous pollutants to microorganisms. Crit Rev Microbiol 8: 99–145.
10. Wani PA, Khan MS, Zaidi A (2007) Chromium reduction, plant growth-promoting potentials and metal solubilization by Bacillus sp. isolated from alluvial soil. Curr Microbiol 54: 237–243.
11. Raskin I, Ensley BD (2000) Phytoremediation of toxic metals; using plants to clean up the environment. John Wiley and Sons New York.
12. Callender E (2003) Heavy Metals in the Environment-Historical Trends. In: Lollar BS, editors. Environmental Geochemistry. Treatise on Geochemistry. Elservier-Pergamon, Oxford. 67–105.
13. Sterckeman T, Douay F, Proix N, Fourrier H (2000) Vertical distribution of Cd, Pb and Zn in soils near smelters in the North of France. Environ Pollut 107: 377–389.
14. Petrouleas V, Crofts AR (2005) The iron-quinone acceptor complex. In: Photosystem II. The light-driven water:plastoquinone oxidoreductase. Wydrzynski T Satoh K, editors. Springer Dordrecht The Netherlands. 177–206.
15. Guskov A, Kern J, Gabdulkhakov A, Broser M, Zouni A, et al. (2009) Cyanobacterial photosystem II at 2.9-angstrom resolution and the role of quinones, lipids, channels and chloride. Nat Struct Mol Biol 16: 334–342.

16. Jursinic P, Warden J, Govindjee (1976) Major site of bicarbonate effect in system-II reaction evidence from ESR signal-IIvf, fast fluorescence yield changes and delayed light-emission. Biochim Biophys Acta 440: 322–330.
17. Robinson HH, Eaton-Rye JJ, van Rensen S, Govindjee (1984) The effects of bicarbonate depletion and formate incubation on the kinetics of oxidationreduction reactions of the Photosystem II quinone acceptor complex. Z Naturforsch C 39: 382–385.
18. Eaton-Rye JJ, Govindjee (1988) Electron-transfer through the quinone acceptor complex of Photosystem-II after one or 2 actinic flashes in bicarbonate-depleted spinach thylakoid membranes. Biochim Biophys Acta 935: 248–257.
19. Farineau J, Mathis P (1983) Effect of bicarbonate on electron transfer between plastoquinones in Photosystem II. In: Inoue Y, Crofts AR, Govindjee, Murata N, Renger G, Satoh K, editors. The oxygen evolving system of photosynthesis. Academic Press Inc. 317–325.
20. Van Rensen JJS, Tonk WJM, Debruijn SM (1988) Involvement of bicarbonate in the protonation of the secondaryquinone electron-acceptor of Photosystem II via the nonheme iron of the quinone–iron acceptor complex. FEBS Lett 226: 347–351.
21. Renger G (2011) Light induced oxidative water splitting in photosynthesis: Energetics, kinetics and mechanism. J Photochem Photobiol B 104: 35–43.
22. Qufei L, Fashui H (2009) Effects of Pb^{2+} on the structure and function of photosystem II of Spirodela polyrrhiza. Biol Trace Element Res 129: 251–260.
23. Boucher N, Carpentier R (1999) Hg^{2+}, Cu^{2+}, and Pb^{2+}-induced changes in photosystem II photochemical yield and energy storage in isolated thylakoid membranes: A study using simultaneous fluorescence and photoacoustic measurements. Photosynth Res 59: 167–174.
24. Rashid A, Popovic R (1990) Protective role of $CaCl_2$ against Pb^{2+} inhibition in Photosystem II. FEBS Lett 271: 181–184.
25. Belatik A, Hotchandani S, Tajmir-Riahi HA, Carpentier R (2013) Alteration of the structure and function of photosystem I by Pb^{2+}. J Photochem Photobiol B In Press.
26. Joly D, Bigras C, Harnois J, Govindachary S, Carpentier R (2005) Kinetic analyses of the OJIP chlorophyll fluorescence rise in thylakoid membranes. Photosynth Res 84: 107–112.
27. Ducruet JM (2003) Chlorophyll thermoluminescence of leaf discs: simple instruments and progress in signal in interpretation open the way to new ecophysiological indicators. J Exp Bot 54: 2419–2430.
28. Gauthier A, Govindachary S, Harnois J, Carpentier R (2006) Interaction of N,N,N′,N′-tetramethyl-p-phenylenediamine with photosystem II as revealed by thermoluminescence: reduction of the higher oxidation states of the Mn cluster and displacement of plastoquinone from the QB niche. Biochim Biophys Acta 1757**:** 1547–1556.
29. Rajagopal S, Egorova EA, Bukhov NG, Carpentier R (2003) Quenching of excited states of chlorophyll molecules in submembrane fractions of photosystem I by exogenous quinones. Biochim Biophys Acta 1606: 147–152.
30. Putrenko II, Vasiliev S, Bruce D (1999) Modulation of flash-induced photosystem II fluorescence by events occurring at the water oxidizing complex. Biochemistry 38: 10632–10641.
31. Ono TA, Noguchi T, Nakajima Y (1995) Characteristic changes of function and structure of photosystem II during strong light photoinhibition under aerobic conditions. Biochim Biophys Acta 1229: 239–248.
32. Strasser RJ, Govindjee (1992) On the O–J–I–P fluorescence transients in leaves and D1 mutants of Chlamydomonas reinhardtii. In: Murata N, editors. Research in Photosynthesis, Kluwer Academic Publishers Dordrecht The Netherlands. 23–32.
33. Strasser RJ, Srivastava A, Govindjee (1995) Polyphasic chlorophyll a fluorescence transient in plants and cyanobacteria. Photochem Photobiol 61: 32–42.
34. Bukhov NG, Egorova EA, Govindachary S, Carpentier R (2004) Changes in polyphasic chlorophyll a fluorescence induction curve upon inhibition of donor or acceptor side of photosystem II in isolated thylakoids. Biochim Biophys Acta 1657: 121–130.
35. Pospisil P, Dau H (2002) Valinomycin sensitivity proves that light-induced thylakoid voltages result in millisecond phase of chlorophyll fluorescence transients. Biochim Biophys Acta 1554: 94–100.
36. Boisvert S, Joly D, Carpentier R (2006) Quantitative analysis of the experimental O–J–I–P chlorophyll fluorescence induction kinetic apparent activation energy and origin of each kinetic step. FEBS J 273: 4770–4777.
37. Joly D, Carpentier R (2007) The oxidation/reduction kinetics of the plastoquinone pool controls the appearance of the I-peak in the O–J–I–P chlorophyll fluorescence rise: Effects of various electron acceptors. J Photochem Photobiol B 88: 43–50.
38. Barazzouk S, Kamat P, Hotchandani S (2005) Photoinduced electron transfer between chlorophyll a and gold nanoparticles. J Phys Chem 109: 716–723.
39. Anderson JM, Park YI, Soon WS (1998) Unifying model for the photoinactivation of Photosystem II in vivo under steady-state photosynthesis. Photosynth Res 56: 1–13.
40. Lazar D (2006) The polyphasic chlorophyll a fluorescence rise measured under high intensity of exciting light Funct Plant Biol 33: 9–30.
41. Babani F, Lichtenthaler HK (1996) Light-induced and age-dependent development of chloroplasts in etiolated barley leaves as visualized by determination of photosynthetic pigments, CO_2 assimilation rates and different kinds of chlorophyll fluorescence ratios. J Plant Physiol 148: 555–566.
42. Putrenko II, Vasiliev S, Bruce D (1999) Modulation of flash-induced photosystem II fluorescence by events occurring at the water oxidizing complex. Biochemistry 38: 10632–10641.
43. Pospisil P, Tyystjärvi E (1999) Molecular mechanism of high temperature-induced inhibition of acceptor side of photosystem II. Photosynth Res 62: 55–66.
44. Mamedov F, Stefanson H, Albersson PA, Styring S (2000) Photosystem II in different parts of the thylakoid membrane: a functional comparison between different domains. Biochemistry 39: 10478–10486.
45. Mamedov F, Rintamaïki E, Aro EM, Andersson B, Styring S (2002) Influence of protein phosphorylation on the electron-transport properties of Photosystem II. Photosynth Res 74: 61–72.
46. Vass I, Govindjee (1996) Thermoluminescence from the photosynthetic apparatus. Photosynth Res 48: 117–126.
47. Sane PV (2004) Thermoluminescence: a Technique for Probing Photosystem II. In: Carpentier R, editors. Photosynthesis Research Protocols Humana Press. Totova New Jersey USA. 229–248.
48. Rutherford AW, Crofts AR, Inoue Y (1982). Thermoluminescence as a probe of photosystem II photochemistry the origin of the flash-induced glow peaks. Biochim Biophys Acta 682: 457–165.
49. Belatik A, Essemine J, Hotchandani S, Carpentier R (2012) Afterglow thermoluminescence band measured in isolated chloroplasts. Photochem Photobiol 88: 67–75.
50. Ducruet JM, Roman M, Ortega JM, Janda T (2005) Role of the oxidized secondary acceptor Q_B of photosystem II in the delayed afterglow chlorophyll luminescence. Photosynth Res 84: 161–166.
51. Demeter S, Vass I. (1984) Charge accumulation and recombinaition in photosystem II studied by thermoluminscence. Participation of the primary acceptor Q and secondary B in the generation of thermoluminescence in chloroplasts. Biochim Biophys Acta 764: 24–32.
52. Rebeiz CA, Castelfranco PA (1973) Protochlorophyll and chlorophyll biosynthesis in cell-free systems from higher plants. Ann Rev Plant Physiol 24: 129–72.
53. Wu JT, Lorenzen H (1984) Effect of copper on photosynthesis in synchronous Chlorella cells. Bot Bull Acad Sinica 25: 125–32.
54. Wu X, Liau C, Chunxiang Q, Hao H, Xianqing L, et al. (2008) Effects of lead on activities of photochemical reaction and key enzymes of carbon assimilation in spinach chloroplast. Biol Trace Element Res 126: 269–279.
55. Kruger GHJ, Tsimilli-Michael M, Strasser RJ (1997) Light stress provokes plastic and elastic modifications in structure and function of Photosystem II in camellia leaves. Plant Physiol 101: 265–277.
56. Boisvert S, Joly D, Carpentier R (2006) Quantitative analysis of the experimental O-J-I-P chlorophyll fluorescence induction kinetics: Apparent activation energy and origin of each kinetic step. FEBS J 273: 4770–4777.
57. Joly D, Carpentier R (2007) The oxidation/reduction kinetics of the plastoquinone pool controls the appearance of the I-peak in the O-J-I-P chlorophyll fluorescence rise: Effects of various electron acceptors. J Photochem Photobiol B 88: 43–50.
58. Schmidt W, Neubauer C, Kolbowski J, Schreiber U, Urbach W (1990) Comparaison of effects of ar pollutants (SO_2, O_3, NO_2) on intact leaves by measurement of chlorophyll fluorescence and P700 absorbance changes. Photosynth Res 25: 241–248.
59. Gauthier A, Joly D, Boisvert S, Carpentier R (2010) Period-four modulation of photosystem II primary quinone acceptor (Q_A) reduction/oxidation kinetics in thylakoid membranes. Photochem Photobiol 86: 1064–1070.
60. Mohanty N, Vass I, Demeter S (1989) Impairment of photosystem II activity at the level of secondary quinone electron acceptor in chloroplasts treated with cobalt, nickel and zinc ions. Physiol Plant 76: 386–390.
61. Yruela I, Gatzen G, Picorel R, Holzwarth AR (1996) Cu(II)-inhibitory effect on Photosystem II from higher plants. A picoseconds time-resolved fluorescence study. Biochemistry 35: 9469–9474.
62. Sigfridsson KGV, Bernat G, Mamedov F, Styring S (2004) Molecular interference of Cd^{2+} with photosystem II. Biochim Biophys Acta 1659: 19–31.
63. Krieger A, Weis E, Demeter S (1993) Low pH-induced Ca^{2+} ion release in the water-splitting system is accompanied by a shift in the midpoint redox potential of the primary quinone acceptor Q_A. Biochim Biophys Acta 1144: 411–418.
64. Boisvert S, Joly D, Leclerc S, Govindachary S, Harnois J, et al. (2007) Inhibition of the oxygen-evolving complex of photosystem II and depletion of extrinsic polypeptides by nickel. Biometals 20: 879–889.
65. Beauchemin R, Gauthier A, Harnois J, Boisvert S, Govindachary S, et al. (2007) Spermine and Spermidine inhibition of photosystem II: Disassembly of the oxygen evolving complex and consequent perturbation in electron donation from Tyr_z to $P680^+$ and the quinone acceptors Q_A^- to Q_B. Biochim Biophys Acta 1767: 905–912.
66. Homann PH, Madabusi LV (1993) Modification of the thermoluminescence properties of Ca^{2+} depleted photosystem II membranes by the 23 kDa extrinsic polypeptide and by oligocarboxylic acids. Photosynth Res 35: 29–39.
67. Vass I, Ono T, Inoue Y (1987) Stability and oscillation properties of thermoluminescent charge pairs in the O_2-evolving system depleted of Cl^- or the 33 kDa extrinsic protein. Biochim Biophys Acta 892: 224–235.